Poly (Ethylene-vinyl co-vinyl acetate) /Clay nanocomposites: mechanical, morphology and thermal behavior

Susan Joseph*, Walter W Focke
Institute of Applied Materials, Department of Chemistry and Chemical Engineering, University of Pretoria, Lynwood Road, South Africa

---

Nanocomposites of Ethylene-vinyl acetate copolymer (EVAL) with Dellite organoclay were prepared in a laboratory extruder. The extent of intercalation of the nanocomposites was studied by field emission scanning electron microscopy (FESEM) and X-ray diffraction (XRD). It was established that the organoclay is well dispersed and preferentially embedded in the EVAL phase. Further, the intercalation degree of the organoclay decreased with increasing organoclay content. The mechanical properties of the nanocomposites were studied as a function of clay loading and EVAL type. The nanocomposites exhibited enhanced thermal stability as seen in thermogravimetric studies.

Keywords: *nanocomposites; ethylene-vinyl acetate copolymer (EVAL), organoclay, morphology, thermal stability*

***Corresponding author:**
Fax: +27- 12- 420 2516
Tel: +27 - 12 -420 3728 (off)
E-mail address: susanaruvi@gmail.com

INTRODUCTION

The growing interest in the field of nanocomposites originates both from the point of view of fundamental property determination and the development of new materials to meet varied applications. The combination of clay with functional polymers interacting at atomic level paves the basis for preparing inorganic-organic nanostructured materials called polymer-clay nanocomposites [1-5]. The dispersion of filler and the degree of interfacial interaction between filler and matrix directly affect the polymer properties and make a great contribution to a series of properties of the composite materials, even at very low filler concentration [6–9]. Artzi et al. [10] reported higher intercalation level for higher effective clay content. According to Vaia et al. [11], exfoliation results in higher exposed clay surface at higher interaction levels between clay and polymer, which may partially hinder segmental movements. Zhao and coworkers [12] reported that attachment of polymer to the silicate layers are shown to be akin to polymer brushes at the clay surface and promotes compatibility. Many reports are available for the preparation of exfoliated/intercalated polymer nanocomposites by melt intercalation method [12-13].

EVA/ clay-based nanocomposites have received widespread attention due to the possibility of tailoring their strength/stiffness/toughness balance as well as improving the thermal stability, stress-crack resistance and gas barrier characteristics. The enhanced barrier properties combined with good transparency will make them ideal packaging materials. Ethylene-vinyl acetate copolymer (EVAL) is a unique matrix polymer for nanocomposites because of the strong interactions it develops with the clay. Many reports are available on composites of organoclay with EVA [14–24]. Increase in property in these nanocomposites is due to interactions of polar –OH groups that exists on the clay surface with polar functional groups of EVA, which are capable of strong intermolecular interactions [22]. Zhang et al. [23] have reported that the properties of EVA/clay nanocomposites are dependent on the effects of clay contents and vinyl acetate contents of EVA. The prior works are difficult to compare because of the diversity of test procedures, processing equipments and clay materials adopted by various researchers. The present work is focused on the systematic examination of the effects of Dellite 72T nanoclay on two grades of EVAL with different melt flow indices. The clay dispersion and morphology of the nanocomposites were investigated using XRD and FESEM.The mechanical and thermal stability properties of the nanocomposites were also investigated.

EXPERIMENTAL

Materials

The two grades of EVAL employed are EVAL -250 and EVAL -210. They are commercial products, polyethylene-co- vinyl acetate copolymers, supplied by DuPont, USA.EVAL is cheap and offers a wide range of high-melt flow indices, low melting temperatures and in addition, its good compatibility makes it an ideal polymer that can be compounded with nanoclays. The material characteristics are listed in Table 1. The commercial organoclay, Dellite 72T supplied by Laviosa Chemicals, Italy was used in the study. Dellite 72T is montmorillonite, modified by ditallow dimethyl ammonium ion. The bulk density reported is 0.45 kg/m^3, loss at ignition, 37-41%, d-spacing 2.9 nm and particle size after dispersion, 500nm.

TABLE 1. Materials used in this study.

Material characteristics	**EVAL-250**	**EVAL -210**
Density, kg/m^3	0.951	0.951
MFI (dg/min @ 190°C/2, 16 kg)	25	400
T.S , ASTM D1708	11 MPa	~2.8 MPa
Vinyl acetate content.	28 mol%	28 mol%
Softening point	127°C	82°C

Nanocomposite preparation

EVAL pellets were dried in vacuum at 70°C for a minimum of 12 hours prior to compounding while the organoclay was used as received. In this work, the master batches of EVAL with 20 wt% clay was prepared by processing in a two-roll mill at 42 revolutions per minute for approximately 40 minutes. The temperature of mixing was 180°C for both the nanocomposites. The master batches were thereafter diluted in a required amount by adding EVAL to get the corresponding compositions by premixing

and then melt mixing in a cavity transfer molder (CTM). Filaments of the composite produced were ground and then formed into extrudable pellet specimens by injection-molding machine (Engel) with ASTM standard mold. Prior to extrusion, all mixes were dehumidified in vacuum oven (70ºC for 8 hours). Composites with varying filler levels (1, 3, 5 and 10 wt%) were prepared.

X-ray diffraction

X-ray diffraction (XRD) was used to characterize the formation of the nanocomposite. XRD patterns were recorded with a PANanalytical X'pert diffractometer equipped with Ni-filtered Co Kα radiation (λ was 0.17903 nm) under 40 kV voltage and a 40 mA current. The scanning rate employed was $18min^{-1}$. The samples were investigated over a diffraction angle (range of 0-10) at ambient temperature. The clay was analyzed as powder and the composites as disks of 4 mm thickness and 20mm diameter.

The Phase morphology

The microstructure of the blends was observed with a field emission scanning electron microscope (FESEM), Zeiss Ultra 55 at 60 kV. Thin block of sample was cut from the specimens and polished well, mounted on suitable sample holders to observe through FE scanning electron microscope. Multiple images from various locations at different magnifications were collected to provide an overall assessment of dispersion. The sample preparation for FESEM is much easier and has got minimum sample charging damage when compared to the cumbersome sample preparation in transmission electron microscopy (TEM).

Mechanical properties

The static mechanical features of the nanocomposites were performed by tensile measurements at ambient conditions according to ASTM D638 type V method using Instron tensile tester in uniaxial tension mode equipped with digital data acquisition capabilities. The punched dog- bone samples cut along the machine direction was used. Five replicates of each were tested at an extension rate of 50 mm/min. The Young's modulus was determined from the stress-strain curves.

Thermal properties

Thermogravimetric measurements were performed under air flow using Mettler Toledo Star System instrument with approximately 15 mg samples, heating from 25°C to 900°C at flow rate of 50 ml/min. A constant heating rate of 10°C/min was maintained. TGA data collection for all the nanocomposites was made under identical conditions. The thermal stability characterization of degradation temperature (Td) was ascribed to the peak position of DTG peak. TGA results include temperature values at 10% weight loss (T10) that gives a relative measure of the onset of degradation, temperature at 50% weight loss (T50) the middle weight %, and the residue remaining at 150 and 900°C.

RESULTS AND DISCUSSION

XRD

The space gallery for the clays and the mean spacing between clay silicate layers in EVAL nanocomposites were determined using the Bragg's law. Figure 1 shows the

scattering intensity profiles of EVAL-250 based nanocomposites. The XRD data of Dellite 72 T clay is also shown in the figure as standard data. X-ray diffraction of the nanocomposites clearly indicates the intercalation of EVA macromolecules into the MMT gallery space, increasing interlayer distance from 2.62 nm to about 3.58 nm (37% increase).It means that no true exfoliation occurs and MMT layers remain in the stack form, though swelled with polymer. Peak at ~ 5 degree is due to secondary reflections. The secondary reflections become more pronounced in the high loading, indicating the existence of more clay in the material. There is apparently little difference in the d-spacing on varying the clay concentration. This indicates a percolation threshold in the material. With high surface area associated with clays, it is expected that even small amounts of the nanofillers can have significant effects [25]. Chemical modification of clays enhances the d spacing between clay nano layers. According to Dennis et al. [26] during melt-mixing, fracturing process of the organoclay takes place first; that is, external layers are subjected to dynamic high shear forces that ultimately cause their delamination from the stack of layers building the organoclay particles, and then an onion-like delamination process continues to disperse the layers of silicate into the polymer matrix. Cho and Paul [27] proposed a model relating intercalation and exfoliation for melt-processed nanocomposites in which they envision that polymer diffuses into the galleries, thereby increasing the d-spacing; however, some of the polymer tails remain entangled in the bulk of the matrix. Table 2 lists a summary of XRD analysis of the nanocomposites. Since a detectable shifting of diffraction angle was observed towards a lower angle, it was reasonable to conclude that few chains of EVAL have penetrated through the silicate layers, suggesting that the clay remain ordered.

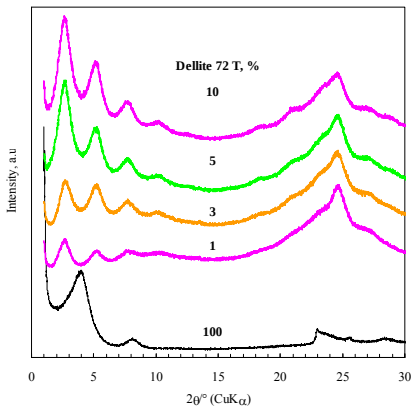

Figure 1. XRD patterns of organophilic clay (Dellite 72T), and EVAL/clay nanocomposites. The diffraction patterns were arbitrarily shifted along the Y-axis to facilitate viewing.

Figure 2 shows XRD profiles of EVAL-210/Dellite 72T nanocomposites. The basal spacing of clay in the composites measured by XRD verified an increased gallery height of 1.30 nm for the clay in the 1wt% composites indicating intercalated nanoclay dispersion for EVAL-210. At 3% clay loading, the peaks are shifted to lower as well as higher angles. The shifting to higher angles is due to matrix amorphousness. The greatest layer swelling is given by 1wt% sample. This indicates that lower loading of clay is more favorable for intercalation of polymer chains into EVA matrix. The increase in d-spacing

for the polymer nanocomposites relative to organoclay show that the silicate layers have expanded because of intercalation of polymer chains into gallery spaces.

TABLE 2. The d -spacing values in EVAL/clay nanocomposites.

Sample	diffraction angle(°)	d-spacing(nm)	Δd_{001}(nm)
Dellite 72T	3.99	2.62	-
EVAL 250-1% 72T	2. 87	3.58	0.96
EVAL 250-3% 72T	2.84	3.89	1.27
EVAL 250-5% 72T	2.73	3.75	1.13
EVAL 250-10% 72T	2.64	3.57	0.95
EVAL 210-1% 72T	2.62	3.92	1.30
EVAL 210-3% 72T	2.65	3.86	1.24

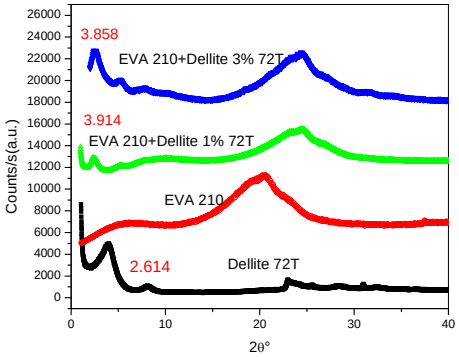

Figure 2. XRD patterns of unmodified EVA 210, organophilic clay (Dellite 72T), and EVA/clay nanocomposites. The diffraction patterns were arbitrarily shifted along the Y- axis to facilitate viewing.

Morphology

Figures 3 (a) and (b) give the FESEM images of the EVAL-250 and EVAL- 210 nanocomposite containing 3 wt% clay respectively. One can easily recognize that clay is finely and rather uniformly distributed in the related matrices with a clear definition of the layered structure in intercalated clay. Since clay has much higher electron density, the dark lines are the cross section of the clay layers that have been delaminated and dispersed in the polymer matrices, while the light lines represent the matrix polymer. In the micrographs presented in figures, some orientation of the nanoclay particles can be observed. It can be seen that the average d-spacing of 72T in modified EVAL- 250 nanocomposites indicates an ordered intercalated structure due to the fact that the separation between the intercalated nanolayers is uniform as seen in the figure 3(a). It is expected to be induced by compression flow of the nanomaterials during compression molding. Similar studies for bismaleimide-organoclay nanocomposites have been made by Meng and Hu [28]. The figures indicate that 3% of clays can be easily intercalated in the EVAL matrix. If the number of large clay tactoids observed decreases by comparing

two different clay samples, then the samples with less clay tactoids is presumed to have better dispersion [29]. FESEM observations depict that the number of clay layers in the clay stacks in EVAL-250/72T NC is smaller than that in case of EVAL-210/72T NC and a much more homogeneous distribution of the nanoparticles. The FESEM investigation revealed the presence of the nano sized inclusions around 80 nm. Similar is the observation with EVAL-210/ Dellite 72T nanocomposite. This finding is consistent with the nanofiller concentration dependencies of the inter-gallery height of the nanocomposites already discussed.

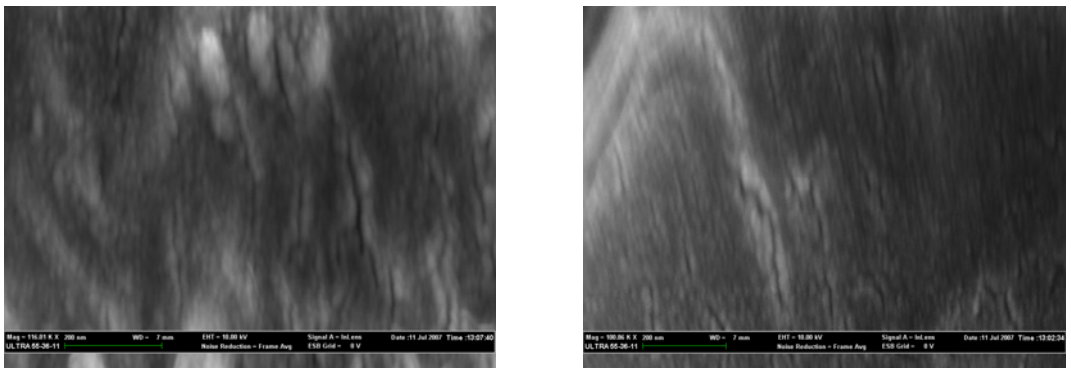

(a) **(b)**

Figure 3. FESEM micrographs of (a) EVA-250 and (b) EVA-210 nanocomposites containing 3% Dellite 72T.

Mechanical properties

Table 3 summarizes the mechanical data for selected EVAL-250 nanocomposites. Clay incorporation slightly improved the tensile properties. The composites exhibited slight improvement of tensile modulus over its pristine counterpart. It is considered, that high aspect ratio of the layers, large contact area with the matrix could be responsible for tensile property enhancement. It is well known that the filler particles reduce the molecular mobility of polymer chains, resulting in a less flexible material with a higher tensile modulus. Furthermore, the final conversion of the nanocomposite increased with increasing clay content, resulting in a higher crosslinking density of the polymer matrix with a high tensile strength. Further addition of organoclay resulted in severe material embrittlement as reflected in a drop of both tensile strength and strain values. The strong EVA/clay interactions are responsible for the unique behavior of the nanocomposites [30]. Surprisingly, Young's modulus of the composite is substantially increased with increase in organoclay content (about 183% higher than neat EVAL), which slightly reduces the elongation at break (Table 3). The most significant increase in modulus occurs with the addition of 10 wt% clay. This conveys stiffness enhancement upon addition of filler.The increased performance is a result of intercalation of nano-size silicate sheets from larger aggregate particles that greatly increased the surface area of interaction between clay and the matrix. It is common for the polymeric material that better the tensile strength, the poorer the elongation-at-break. But for some polymer nanocomposites this kind of unexpected abnormal behavior in physical properties can be observed [31].

TABLE 3. Mechanical data of EVAL-250 nanocomposites.

Sample	T.S. (MPa)	Y.M. (MPa)	Eb%
EVAL 250	4.05	7.1	454
EVAL 250-1% 72T	4.10	7.8	483
EVAL 250-3% 72T	4.13	10.9	473
EVAL 250-5% 72T	4.46	15.8	475
EVAL 250-10% 72T	3.80	20.1	391

TABLE 4. Mechanical data of EVAL-210 nanocomposites.

Sample	T.S.(MPa)	Y.M.(MPa)	Eb%
EVAL 210	1.62	3.96	374
EVAL 210-1% 72T	1.68	4.2	427
EVAL 210-3% 72T	1.70	5.0	508
EVAL 210-5% 72T	1.70	5.0	509

Table 4 summarizes the mechanical data of virgin EVAL-210 and its nanocomposites. There is only marginal increase in tensile strength, tensile moduli and Eb% with clay loading. Figure 4 is a comparative plot of the tensile strength for the EVAL- 250 and 210 nanocomposites as a function of clay loading, clearly revealing highest values in tensile strength at 5% clay loading for the EVAL -250 nanocomposites.The improvement in mechanical properties for EVAL-250/72T NC can be accounted by the FESEM observations that the number of clay layers in the clay stacks in EVAL-250/72T NC is smaller than that in case of EVAL-210/72T NC. Mechanical observations corroborates the XRD data. XRD Inclusions of particles with higher modulus than that of the matrix always increases the nanocomposites' initial resistance against applied stress. Mechanical measurements indicated that the clay content has comparatively higher influence on modulus than on strength.

Table 5. TGA results of organoclays, EVAL 250 and EVAL 210/clay nanocomposites.

Sample	Residue at		DTG (°C)	T_{10}(°)	T_{50}(°C)	Clay residue %
	150°C	900°C				
Dellite 72T	98.6	59.70	293 & 582	290.3	-	63.6
EVAL 250	100	0.72	344 &444	334	433	1.21
EVAL 250-1% 72T	100	1.08	325 & 444	338	454	1.80
EVAL 250-3% 72T	100	2.05	344 & 479	338	465	3.44
EVAL 250-5% 72T	100	4.23	344 & 477	336	460	7.09
EVAL 210	100	0.19	341 & 435	337	447	3.6
EVAL 210-1% 72T	100	2.90	349 & 459	339	448	4.9
EVAL 210-3% 72T	99.3	2.70	349 & 459	340	455	4.5

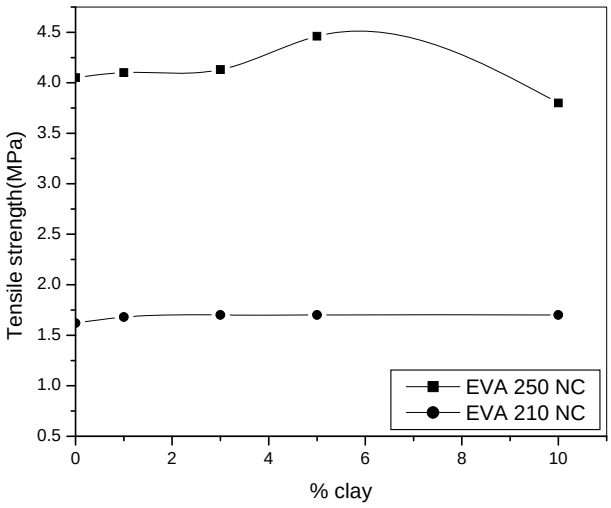

Figure 4 . Comparative plot of the tensile strength for all nanocomposites as a function of clay loading.

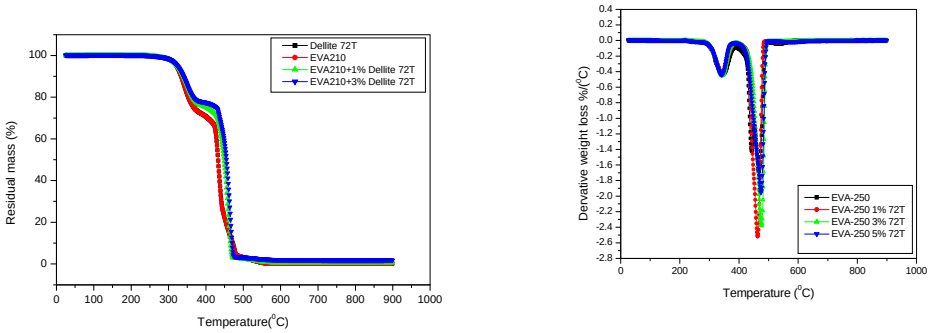

(a) (b)

Figure 5. TG and DTG curves for EVA-210 nanocomposites with and without Dellite 72T clay incorporated.

Thermal stability evaluation by TGA

The TGA curves registered for the EVAL-210 nanocomposites are displayed in Figures 5 (a), (b) show weight loss and derivative weight loss as a function of temperature respectively. All the samples displayed distinct two-step thermal decomposition behavior with distinct mass loss above 340°C. The TGA results for the nanocomposites are quantified in Table 5. The data depicts that clay incorporation increased the temperatures of 10 and 50% weight loss. One can see that clay acted in most nanocomposites as an additional thermooxidative stabilizer. The thermograms in Figure 4 (a) indicate that the nanocomposites show superior degradation stability as compared to EVAL, when the clay content is increased to 3%. This could be attributed to the presence of inorganic content in the form of lamellar intercalated structure that increases the thermal stability of EVAL. Based on the literature data, the mechanism of thermal degradation for EVAL involves two major steps [32-33], (a) the loss of vinyl acetate units via a de-acylation process resulting in the formation of double bonds and (b)

the degradation of resulting partially unsaturated polyethylene material polymer. The presence of hydroxyl groups on the edges of the clay could be the cause of the accelerated initial step. The second degradation step of the composites starts at higher temperatures than that for the neat EVAL as more energy is required to break the additional bonds. This may be attributed to the interfacial interactions between nanoclay and EVAL. Another explanation is due to retardation in evaporation of volatile degradation products as a result of char formation during the first degradation step [34]. The onset temperature of thermal degradation shifts towards a higher value (by ca.50°C) and the content of the solid residue increases substantially for all the nanocomposites. There is apparently little difference in the thermal stabilities on varying the clay concentration. The EVAL- 250 nanocomposite with 5 wt% of organoclay resulted in the highest content of non-volatile residue at temperature from 500ºC- 900ºC. Higher dispersion of the silicate nano layers makes a more efficient obstacle in the process of degradation and, on the other hand, volatilization must also be delayed by the labyrinth effect of the silicate layers dispersed in the nanocomposites [35]. This indicates that thermal degradation delay is mainly due to a decrease in the rate of evolution of the volatile products. Pure EVAL has the highest weight loss. The silicates delay the volatilization of the products originated by carbon-carbon bond scission in the polymer matrix. The increase in Td is related to the increase of dispersion of silicate nanolayers confirmed by FESEM and XRD. The weights remaining after complete polymer decomposition are qualitatively consistent with the fraction of nanoclays present. Quantitatively, however, the values are distinctly low, presumably because most of the well-dispersed nanomaterials are physically lost from the sample as the polymer decomposes. The thermograms of EVAL 210 reveal the same trend for the EVAL-250/clay nanocomposites, except that for EVAL 210 nanocomposites, optimum properties were observed at 1wt% nanoclay concentration.

CONCLUSIONS

Nanocomposites containing Dellite 72T organoclay and two different grades of EVAL (EVAL- 250 and EVAL-210) were prepared by melt intercalation method. Efforts are made to investigate the morphology and properties of the nanocomposites. The diffraction analysis of EVA nanocomposites shows the presence of layered structure that refers to expanded OMMT stacks. The Young's modulus increased marginally for EVA-210 composites, but significantly for the EVA-250 composites. FESEM observation, led to the same conclusions, underlining the good affinity between EVAL and organoclay. The nanocomposites exhibited significantly improved thermal stability due to better interactions between EVAL matrix and nanoclay. The XRD studies, morphological observations, mechanical properties, thermal studies of the nanocomposites are in good agreement. It's worthwhile to note that these results are achieved with only 1-3wt % addition of nanoclay.

ACKNOWLEDGEMENTS

The author (1) would like to acknowledge Institutional Research Development Programme (IRDP) of the NRF, the University of Pretoria and Xyris Technology for financial support for the research work.

REFERENCES

1. A.R. Horrocks, In: D. Price, editor. *Fire Retardant Materials*. Cambridge: Woodhead; (2001).
2. Y. Fukushima, A. Okada, M. Kawasumi, T. Kurauchi, and O. Kamigaito, *Clay Minerals*, **23**, 27(1998).
3. M. Zanetti, S. Lomokin, and G. Camino, *Macromol. Mat. Eng.*, **279**, 1 (2000).
4. S.C. Tjong, *Mater. Sci. Eng.*, **53**, 73(2006).
5. E. Manias, A. Touny, L. Wu, K. Strawhecker, B. Lu, and T.C.Chung, *Chem. Mater*; **13,**3516 (2001).
6. H. Park, A.K. Mohanty, M. Misra, and L.T. Drzal, Presentation in Fall Scientific Meeting, ACS-Midland Section, Michigan (2003).
7. A.Oya, T.J. Pinnavaia, and G.W. Beall (eds), *Polymer-Clay Nanocomposites*, Wiley, London, UK (2000).
8. A.Oya, Y. Kurokawa, and H. Yasuda, *J. Mat. Sci.*, **35**, 1045(2000).
9. M. Alexandre, and Ph.Dubois, *Mater. Sci. Eng.*, **28,** 1(2000).
10. N. Artzi, Y. Nir, D. Wang, M. Narkis, and A. Siegmann, *Polym. Compo.*, **22,** 710 (2001).
11. R.A. Vaia, H. Ishii, and E.P. Giannelis, *Chem. Mater.*, **5,** 1694 (1993).
12. H. Zhao, B.P. Farrell, and D.A. Shipp, *Polymer*, **45,** 4473 (2004).
13. W K. Liang, S. Du, R.N., Q. Zhang, and Fu Qang, *Polymer*, **45,** 7953 (2004).
14. M. Alexandre, G. Beyer, C. Henrist, R. Cloots, A. Rulmont, R. J_er^ome and Ph. Dubois, *Macromol. Rapid Commun.*, **22**, 643(2001).
15. M. Alexandre, G. Beyer, C. Henrist, R. Cloots, A. Rulmont, and R. J_er^ome et al. : *Chem. Mater.,* **13**, 3830 (2001).
16. M. Zanetti., G. Camino, R. Thomann, and R. M€ulhaupt, *Polymer*, **42**, 4501(2001).
17. Y. Tang, Y. Hu, S.F. Wang, Z. Gui, Z. Chen, and W.C. Fan, *Polym. Degrad. Stab.*, **78,** 555(2002).
18. S.Duquesne, C.Jama, M.Le Bras, R. Delobel, P. Recourt, and J.M. Gloagen, *Comp. Sci. and Technol.*, **63**, 1141(2003).
19. M.N.Muralidharan, S.A. Kumar, and S. Thomas, *J. Memb. Sci.*, **315**, 147(2008).
20. S.A. Kumar, M.G. Kumaran and S. Thomas, *J. Phys. Chem. Part B*, **2**, 4009(2008).
21. N. Artzi, M. Narkis, and A. Siegman, *Polym. Eng. Sci.*, **44**, 1019 (2004).
22. A. Sanchez- Solýs, I. Romero-Ibarra, M.R. Estrada, F. Calderas, and O. Manero, *Polym. Eng. Sci.*, **44,** 1094(2004).
23. W. Zhang, D.Chen, Q. Zhao, and Y. Fang, *Polymer*, **44**, 7953(2003).
24. S.B.Misra, and A.S. Lyut, *eXPRESS Polym. Lett.*, **2**, 256(2008).
25. A. Jain, J.S. Gutmann, C.B.W. Garcia, M. Zhang, M.W.Tate, S.M. Gruner, and U. Wiesner, *Macromolecules*, **35**, 4862 (2000).
26. J.W.Cho, D.R. Paul, D.L. Hunter, H.R. Dennis, D. Chang, and S. Kim, *Polymer*, **42**, 9513 (2001).
27. J.W. Cho, and D.R. Paul, *Polymer*, **42**, 1083(2001).
28. J. Meng, and X. Hu, *Polymer*, **45,** 9011(2004).
29. A.B. Morgan, and J.W. Gilman, *J. of Appl. Polym. Sci.*, **87**, 1329 (2003).
30. N. Artzi, M. Narkis and A. Siegmann, *Polym. Eng. Sci.*, **44,** 1019(2004).

31. L. Keller, C. Decker, S. Benfarhi, and K. Zahouily, *Polymer*, **45**, 7437(2004).
32. B.B. Troitskii, G.A. Razuvayev, L.V. Khokhlova, and G.N. Bortnikov, *J. Polym. Sci.; Polym. Symposium,* **42**, 1363 (1973), ACS Symposium Series No. 433, Am. Chem. Soc., Washington, DC p. 60 (1990).
33. M. Zanetti, G. Camino, R. Thomann, and R. Mu¨lhaupt, *Polymer*, **42**, 4501(2001).
34. S. Peeterbroeck, M. Alexandre, R. Je r^ome, and P. Dubois, *Polym. Degrad. Stab.,* **90**, 288(2005).
35. J.W.Gilman, T.C.L. Kashivagi, E.P. Giannelis, E. Manias, S. Lomakin, and J.D. Lichtenhan et al. In: M. Le Bras, G. Caniino, S. Bourbigot, R. Delobel, editors. *Fire Retardancy of Polymers*. Cambridge: The Royal Society of Chemistry (1998).